

Supplementary data for

**Unraveling the Photocatalytic Potential of Transition Metal sulfides and selenides
Monolayers for Overall Water Splitting and Photo-corrosion inhibition**

Shafiq Ur Rehman^{a, b}, Junwei Wang^{a, b}, Guixuan Wu^c, Sajjad Ali^d, Jian Xian^{*a, b}, Nasir
Mahmood^{*c}

^a Yangtze Delta Region Institute (Huzhou), University of Electronic Science and Technology of
China, Huzhou 313001, China.

^b School of Materials and Energy, University of Electronic Science and Technology of China,
Chengdu, 611731, China.

^c State key Laboratory of Coal Conversion, Institute of Coal Chemistry, Chinese Academy of
Sciences, Taiyuan, 030001, China.

^d Energy, Water, and Environment Lab, College of Humanities and Sciences, Prince Sultan
University, Riyadh 11586, Saudi Arabia

^e School of Science, RMIT University, 124 La Trobe Street, 3001 Melbourne, Victoria, Australia.

*Corresponding authors Email: jianxian@uestc.edu.cn ; nasir.mahmood@rmit.edu.au

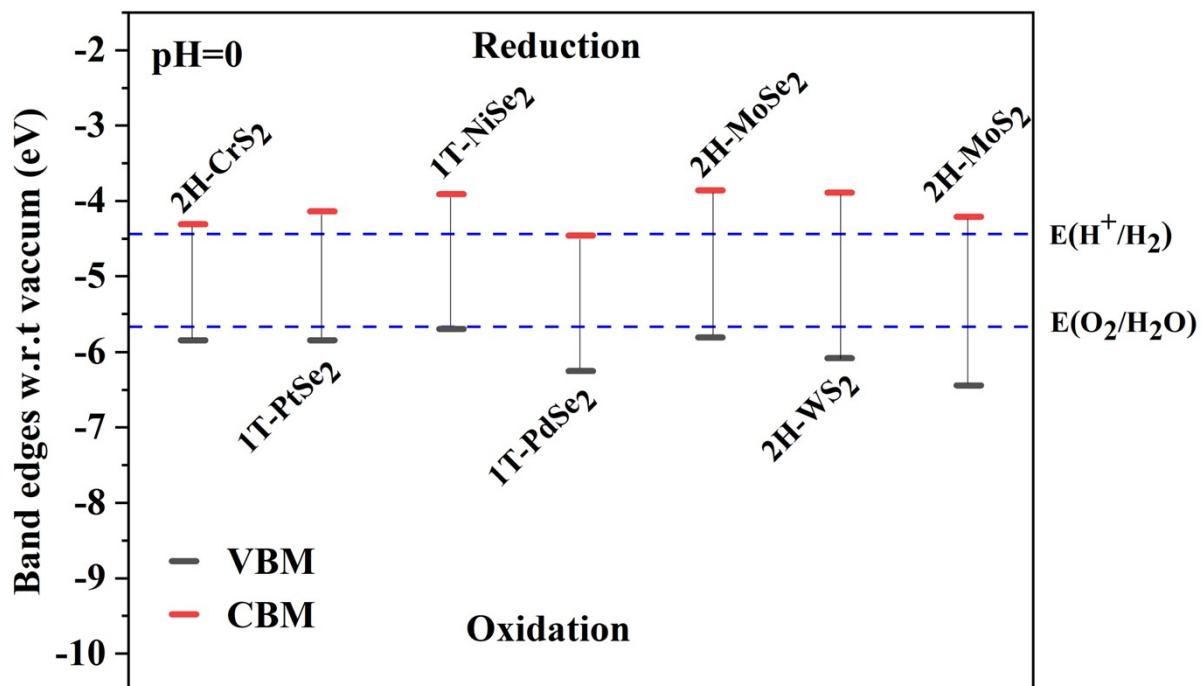


Figure S1. Thermodynamically stable monolayers with suitable CBM (red bars) and VBM (black bars) w.r.t vacuum level for overall water splitting (OWS). The blue dotted lines represent the standard potential for water reduction (-4.45 eV) and oxidation (-5.67 eV) at pH=0.

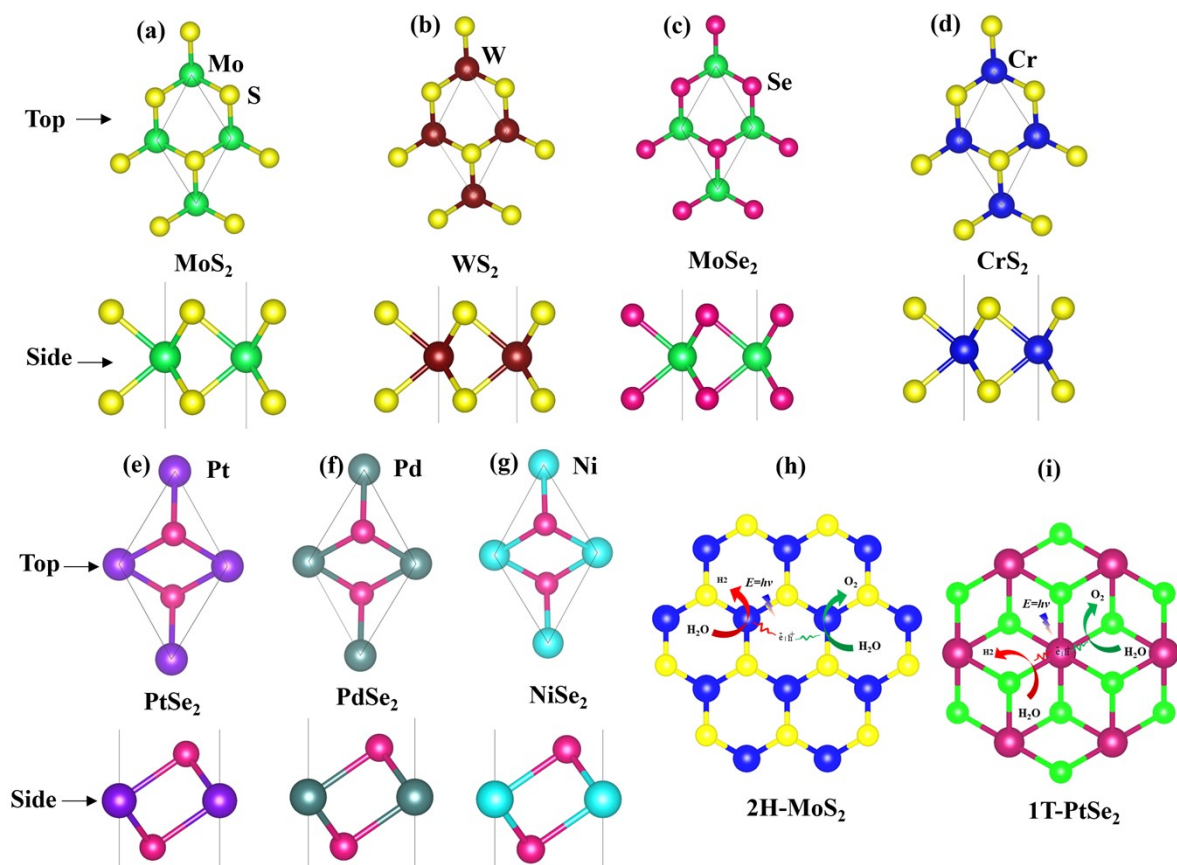


Figure S2. Promising TMSS monolayers with suitable band edge positions for OWS (a-d) Top and side view of MoS₂, WS₂, MoSe₂ and CrS₂ monolayers in 2H phase (e-g) Top and side view of 1T phase PtSe₂, PdSe₂ and NiSe₂ monolayers (h-i) Schematic illustration of OWS reactions on 2H-MoS₂ and 1T-PtSe₂ monolayers without incorporating any co-catalyst.

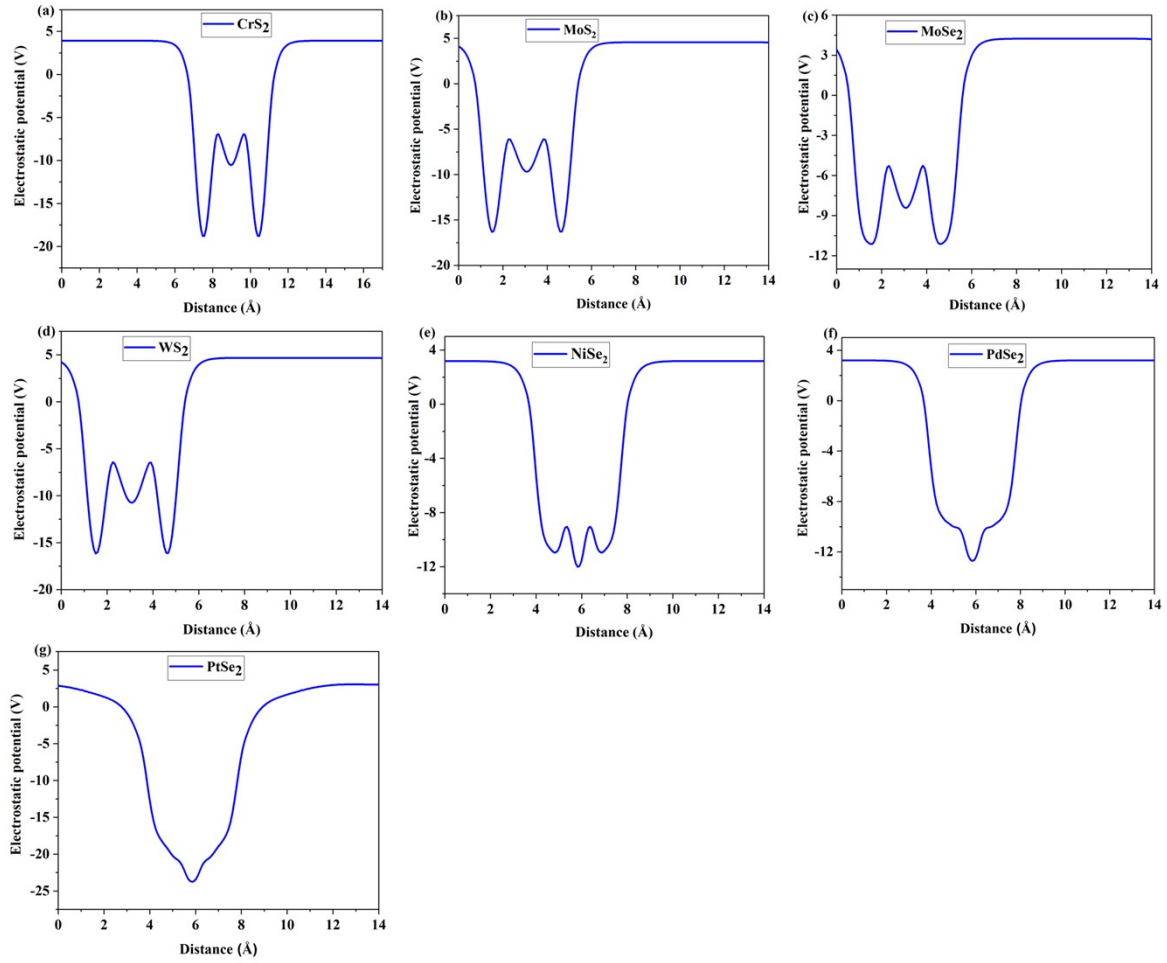


Figure S3. The G_0W_0 based calculated electrostatic potentials for (a-d) CrS_2 , MoS_2 , MoSe_2 , and WS_2 monolayers in 2H phase (e-g) NiSe_2 , PdSe_2 and PtSe_2 monolayers in 1T phase for extracting the conduction band edge (CBM) and valence band edge (VBM) w.r.t the vacuum level.

Table S1 The G_0W_0 calculated CBM, VBM and vacuum level (ϕ_{vac}) of the CrS_2 , MoS_2 , MoSe_2 , WS_2 , NiSe_2 , PdSe_2 and PtSe_2 monolayers are given below.

property	CrS_2	MoS_2	MoSe_2	WS_2	NiSe_2	PdSe_2	PtSe_2
CBM (eV)	-3.44	-3.09	-3.06	-3.26	-4.14	-3.84	-3.65
VBM (eV)	-5.80	-5.75	-5.07	-5.76	-4.92	-5.20	-5.84
ϕ_{vac}	3.91	4.58	4.24	4.68	3.192	3.19	3.32

Table S2. The proposed mechanism for calculating the thermodynamic oxidation and reduction potentials of TMSS monolayers.

System	Reaction equation	$\Delta ZPE-T\Delta S$ ($P_{(gas, atm)}, 10^{-2}-10^{-4}$)	ΔE	Potential	Type
CrS ₂	CrS ₂ +2H ₂ O-> CrO ₂ +2H ₂ +2S	-0.35, -0.46, -0.59	4.02	0.92, 0.89, 0.86	oxidation
	CrS ₂ +2H ₂ -> Cr + 2H ₂ S	-0.17, -0.17, -0.17	1.42	0.31, 0.31, 0.13	reduction
MoS ₂	MoS ₂ +2H ₂ O-> MoO ₂ +2H ₂ +2S	-0.36, -0.46, -0.58	4.38	1.0, 0.98, 0.95	oxidation
	MoS ₂ +2H ₂ -> Mo + 2H ₂ Se	-0.18, -0.18, -0.81	2.05	0.47, 0.47, 0.47	reduction
MoSe ₂	MoSe ₂ +2H ₂ O-> MoO ₂ +2H ₂ +2Se	-0.35, -0.47, -0.59	2.69	0.58, 0.56, 0.53	oxidation
	MoSe ₂ +2H ₂ -> Mo + 2H ₂ Se	-0.17, -0.17, -0.17	2.37	0.55, 0.55, 0.55	reduction
WS ₂	WS ₂ +2H ₂ O-> WO ₂ +2H ₂ +2S	-0.36, -0.46, -0.58	4.08	0.93, 0.87, 0.87	oxidation
	WS ₂ +2H ₂ -> W + 2H ₂ S	-0.18, -0.18, -0.18	1.87	0.42, 0.42, 0.42	reduction
NiSe ₂	NiSe ₂ +2H ₂ O-> NiO ₂ +2H ₂ +2Se	-0.31, -0.43, -0.55	4.79	1.12, 1.09, 1.06	oxidation
	NiSe ₂ +2H ₂ -> Ni + 2H ₂ Se	-0.17, -0.17, -0.17	1.37	0.30, 0.30, 0.30	reduction
PdSe ₂	PdSe ₂ +2H ₂ O-> PdO ₂ +2H ₂ +2Se	-0.33, -0.45, -0.57	6.69	1.59, 1.56, 1.53	oxidation
	PdSe ₂ +2H ₂ -> Pd + 2H ₂ Se	-0.17, -0.17, -0.17	1.08	0.23, 0.23, 0.23	reduction
PtSe ₂	PtSe ₂ +2H ₂ O-> PtO ₂ +2H ₂ +2Se	-0.33, -0.45, -0.57	5.83	1.38, 1.35, 1.32	oxidation
	PtSe ₂ +2H ₂ -> Pt + 2H ₂ Se	-0.17, -0.17, -0.17	1.55	0.35, 0.35, 0.35	reduction

The Gibbs free energy change of reactants and products involved in the proposed mechanism of thermodynamic oxidation and reduction potentials are calculated according to the following equations.

$$\Delta G1 = G(\text{CrO}_2)+2G(\text{H}_2)+2G(\text{S})-G(\text{CrS}_2)-2G(\text{H}_2\text{O}) \quad (1)$$

$$\Delta G2 = G(\text{Cr})+2G(\text{H}_2\text{S})-G(\text{CrS}_2)-2G(\text{H}_2) \quad (2)$$

$$\Delta G3 = G(\text{MoO}_2)+2G(\text{H}_2)+2G(\text{S})-G(\text{MoS}_2)-2G(\text{H}_2\text{O}) \quad (3)$$

$$\Delta G4 = G(\text{Mo})+2G(\text{H}_2\text{S})-G(\text{MoS}_2)-2G(\text{H}_2) \quad (4)$$

$$\Delta G5 = G(\text{MoO}_2)+2G(\text{H}_2)+2G(\text{Se})-G(\text{MoSe}_2) - 2G(\text{H}_2\text{O}) \quad (5)$$

$$\Delta G_6 = G(\text{Mo}) + 2G(\text{H}_2\text{Se}) - G(\text{MoSe}_2) - 2G(\text{H}_2) \quad (6)$$

$$\Delta G_7 = G(\text{WO}_2) + 2G(\text{H}_2) + 2G(\text{S}) - G(\text{WS}_2) - 2G(\text{H}_2\text{O}) \quad (7)$$

$$\Delta G_8 = G(\text{W}) + 2G(\text{H}_2\text{S}) - G(\text{WS}_2) - 2G(\text{H}_2) \quad (8)$$

$$\Delta G_9 = G(\text{NiO}_2) + 2G(\text{H}_2) + 2G(\text{Se}) - G(\text{NiSe}_2) - 2G(\text{H}_2\text{O}) \quad (9)$$

$$\Delta G_{10} = G(\text{Ni}) + 2G(\text{H}_2\text{Se}) - G(\text{NiSe}_2) - 2G(\text{H}_2) \quad (10)$$

$$\Delta G_{11} = G(\text{PdO}_2) + 2G(\text{H}_2) + 2G(\text{Se}) - G(\text{PdSe}_2) - 2G(\text{H}_2\text{O}) \quad (11)$$

$$\Delta G_{12} = G(\text{Pd}) + 2G(\text{H}_2\text{Se}) - G(\text{PdSe}_2) - 2G(\text{H}_2) \quad (12)$$

$$\Delta G_{13} = G(\text{PtO}_2) + 2G(\text{H}_2) + 2G(\text{Se}) - G(\text{PtSe}_2) - 2G(\text{H}_2\text{O}) \quad (13)$$

$$\Delta G_{14} = G(\text{Pt}) + 2G(\text{H}_2\text{Se}) - G(\text{PtSe}_2) - 2G(\text{H}_2) \quad (14)$$

During the free energy calculations in equations (1-14), when reactants and products have different phases (crystal, solution or gas), the phase with the lowest Gibbs free energy under 300 K and 1 bar is considered. Where for the solids the considered temperature is 300K in all energy corrections. All structures for reactants and products are considered in bulk form. The reaction conditions for the calculations of free energies of reactants and products involved in the reduction and oxidation potentials are shown below.

Entity	Temperature (K)	Pressure (atm)	Phase
H ₂ O	300	0.035	liquid
H ₂	300	10 ⁻² -10 ⁻⁴	gas
H ₂ S	300	10 ⁻² -10 ⁻⁴	gas
O ₂	300	0.21	gas
CO ₂	300	0.00039	gas
CH ₂ O ₂	300	10 ⁻² -10 ⁻⁴	liquid

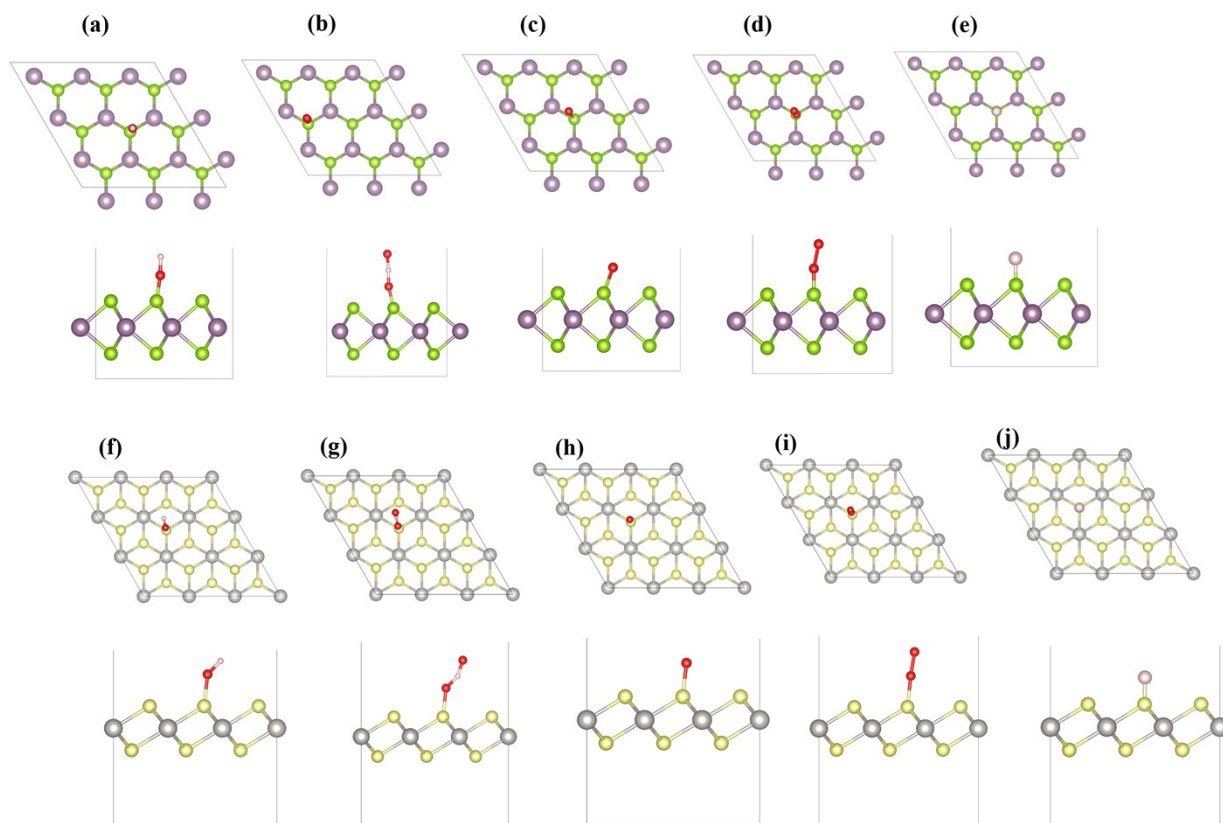


Figure S4. The top and side views of the optimized structures of stable adsorption sites of OH^* , O^* , $O-H-O^*$, O_2^* and H^* intermediates on the surface of $3 \times 3 \times 1$ supercell (a-e) 2H-MoS₂ monolayer (f-j) 1T-PtSe₂ monolayer.